

**Cell Reports, Volume 27**

## **Supplemental Information**

### **Anaerobic Glycolysis Maintains the Glomerular Filtration Barrier Independent of Mitochondrial Metabolism and Dynamics**

**Paul T. Brinkkoetter, Tillmann Bork, Sarah Salou, Wei Liang, Athanasia Mizi, Cem Özel, Sybille Koehler, H. Henning Hagmann, Christina Ising, Alexander Kuczkowski, Svenia Schnyder, Ahmed Abed, Bernhard Schermer, Thomas Benzing, Oliver Kretz, Victor G. Puelles, Simon Lagies, Manuel Schlimpert, Bernd Kammerer, Christoph Handschin, Christoph Schell, and Tobias B. Huber**

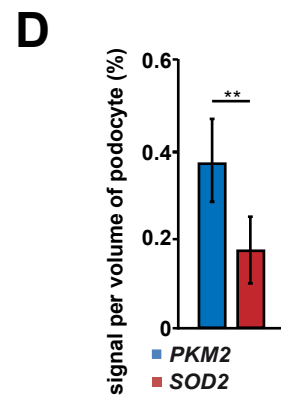
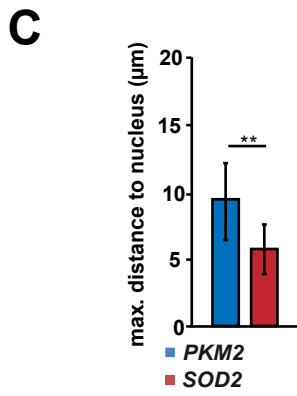
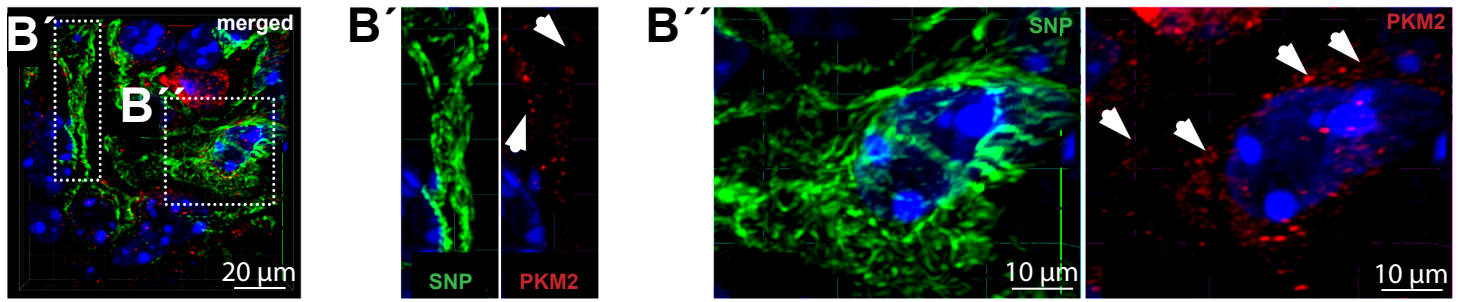
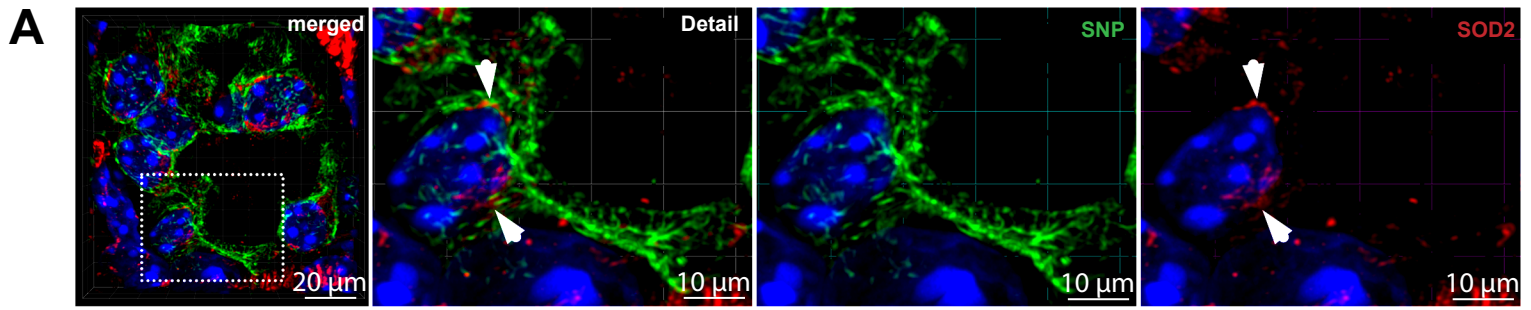


Figure S1: Mitochondria were primarily found within the cytoplasm and primary processes of podocytes, Related to Figure 1

(A) Immunofluorescence image obtained from mouse glomeruli (8 weeks old) for synaptopodin (green, podocyte marker) and SOD2 (red, mitochondrial enzyme). Arrowheads point to mitochondrial signal.

(B) Immunofluorescence image obtained from mouse glomeruli (8 weeks old) for synaptopodin (green, podocyte marker) and PKM2 (red, glycolytic enzyme). Arrowheads in the high magnification point to PKM2 signal, primarily found in foot processes.

(C) Quantification of the maximal distance of SOD2 and PKM2 signal to the nucleus (obtained from 20 glomeruli).

(D) Quantification of the volume of SOD2 and PKM2 signal compared to podocyte volume (obtained from 20 glomeruli).

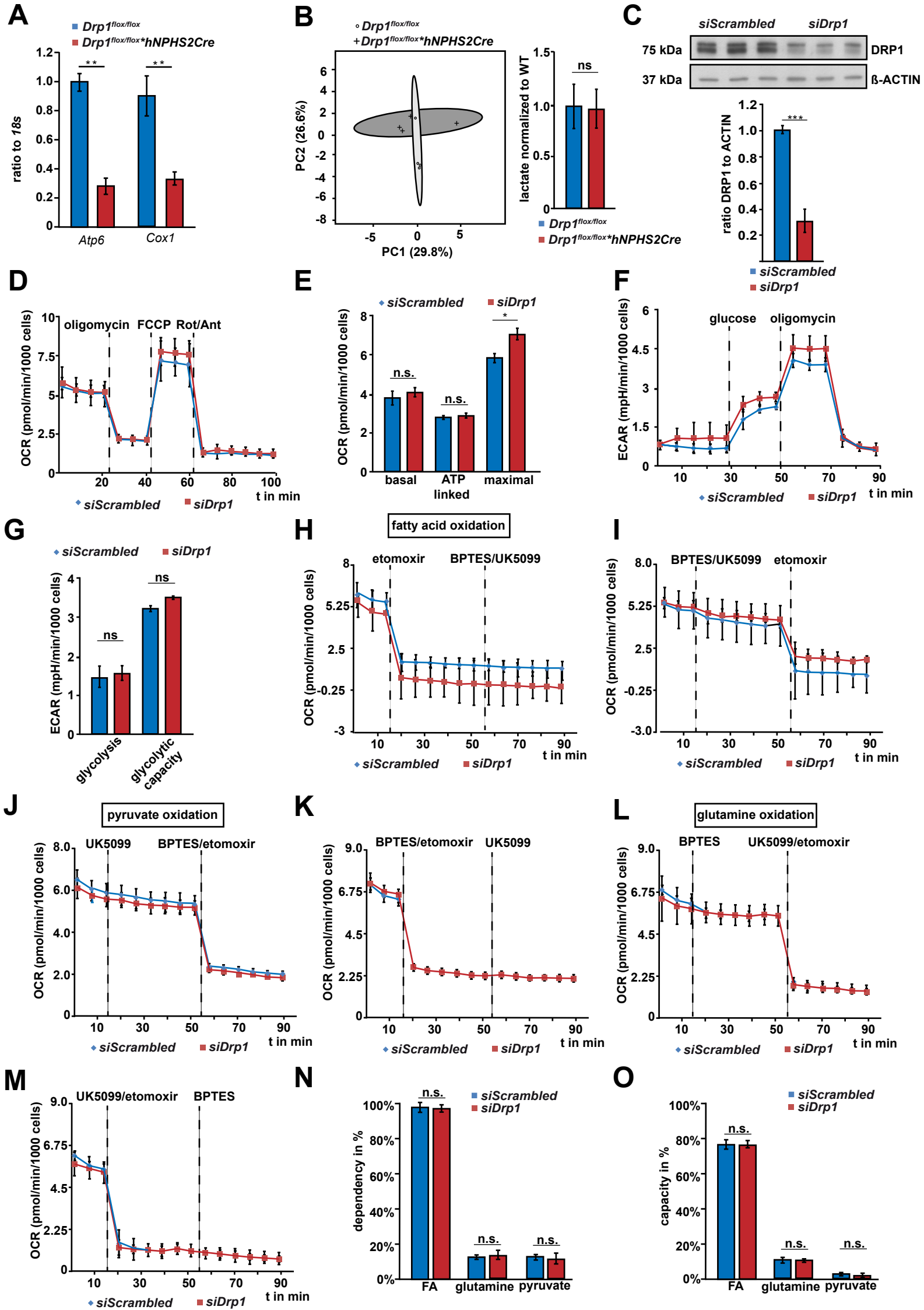


Figure S2: Impact of *Drp1* deletion on the expression of mitochondria encoded genes and function, Related to Figure 4

(A) qPCR for the abundance of mitochondrial DNA (Atp6, Cox I) normalized to genomic DNA (18s) (p-value \*\*  $\leq 0.01$ ).

(B) Principal component analysis of metabolite abundance from kidney cortex obtained from 24-week-old mice of respective genotype assessed by unbiased GC-MS based metabolomic analysis (n=4 each group). Lactate levels normalized to WT.

(C) Western blot and densitometry for the abundance of DRP1 in human podocytes after siRNA-based knock-down compared to scrambled siRNA controls (p-value \*\*\*  $\leq 0.001$ ).

(D) Mitochondrial function of human podocytes after knock-down of *Drp1* and respective controls. Oxygen consumption rate (OCR) was measured at basal level and after the sequential addition of oligomycin (1 mM), FCCP (0.5 mM), and rotenone (Rot; 1.0 mM) + antimycin A (Ant; 1.0 mM; n=3, technical replicates).

(E) Combined results underline the minor role of *Drp1* for mitochondrial respiratory function as shown for basal respiration, ATP-linked oxygen consumption rate and maximal respiratory capacity (p-value \*  $\leq 0.05$ ).

(F) Extracellular acidification rate (ECAR) of human podocytes with knock-down of *Drp1* and respective controls at baseline and after injection of glucose followed by oligomycin.

(G) Combined results underline the minor impact of *Drp1* for anaerobic utilization of glucose as shown for glycolysis and maximal glycolytic capacity.

(H) Dependency of fatty acid oxidation of human podocytes with knock-down for *Drp1* and respective controls obtained after etomoxir and BPTES/UK5099 injection. Final concentrations: etomoxir: 100  $\mu$ M, BPTES: 30  $\mu$ M, UK5099: 30  $\mu$ M.

(I) Capacity of fatty acid oxidation of human podocytes with knock-down for *Drp1* and respective controls obtained after BPTES/UK5099 injection followed by etomoxir, Final concentrations: etomoxir: 100  $\mu$ M, BPTES: 30  $\mu$ M, UK5099: 30  $\mu$ M.

(J) Dependency of pyruvate oxidation of human podocytes with knock-down for *Drp1* and respective controls obtained after UK5099 and BPTES/etomoxir injection. Final concentrations: UK5099: 30  $\mu$ M, etomoxir: 100  $\mu$ M, BPTES: 30  $\mu$ M.

(K) Capacity of pyruvate oxidation of human podocytes with knock-down for *Drp1* and respective controls obtained after BPTES/etomoxir and UK5099 injection. Final concentrations: etomoxir: 100  $\mu$ M, BPTES: 30  $\mu$ M, UK5099: 30  $\mu$ M.

(L) Dependency of glutamine oxidation of human podocytes with knock-down for *Drp1* and respective controls obtained after BPTES and UK5099/etomoxir injection. Final concentrations: BPTES: 30  $\mu$ M, UK5099: 30  $\mu$ M, etomoxir: 100  $\mu$ M.

(M) Capacity of glutamine oxidation of human podocytes with knock-down for *Drp1* and respective controls obtained after UK5099/etomoxir and BPTES injection. Final concentrations: UK5099: 30  $\mu$ M, etomoxir: 100  $\mu$ M, BPTES: 30  $\mu$ M.

(N) Statistics for substrate dependency of human podocytes with knock-down for *Drp1* and respective controls.

(O) Statistics for substrate capacity of human podocytes with knock-down for *Drp1* and respective controls.

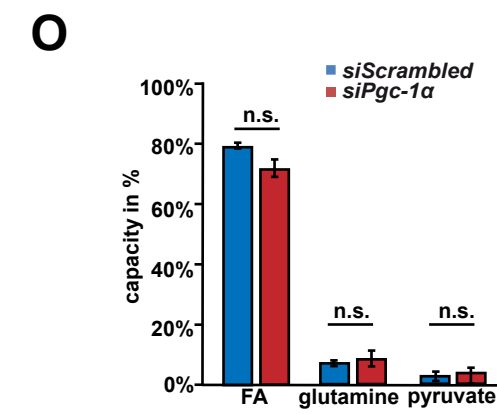
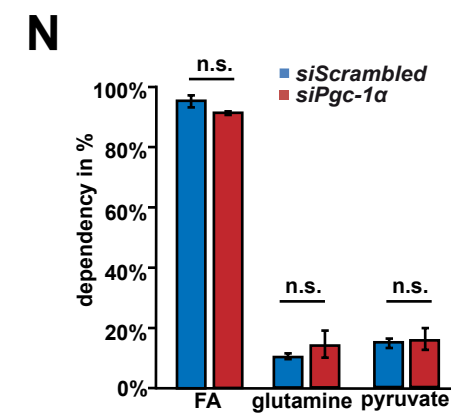
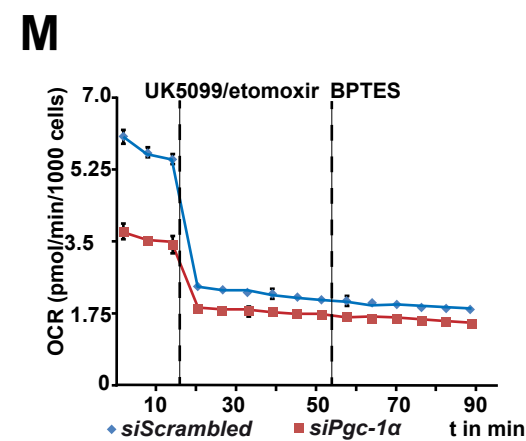
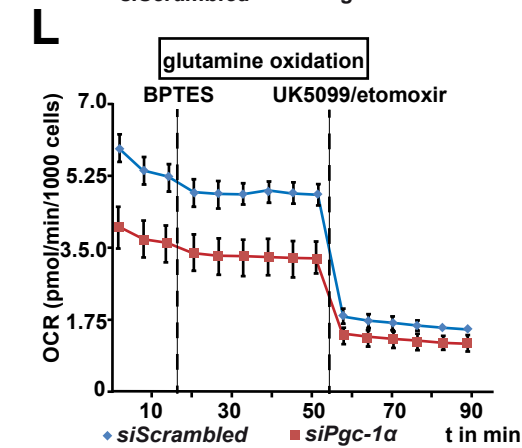
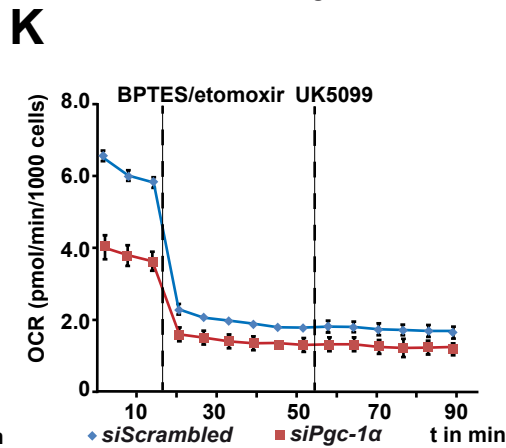
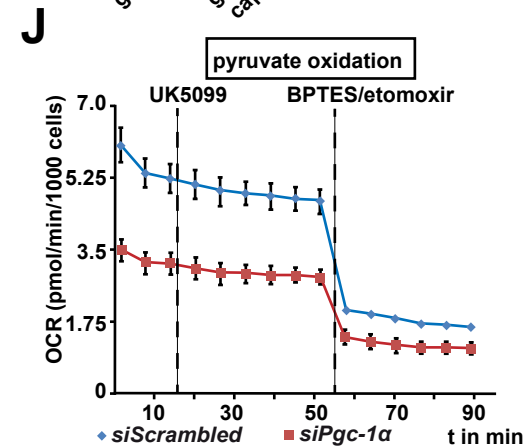
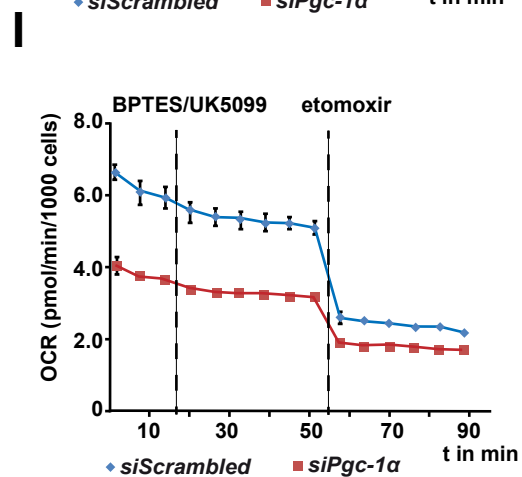
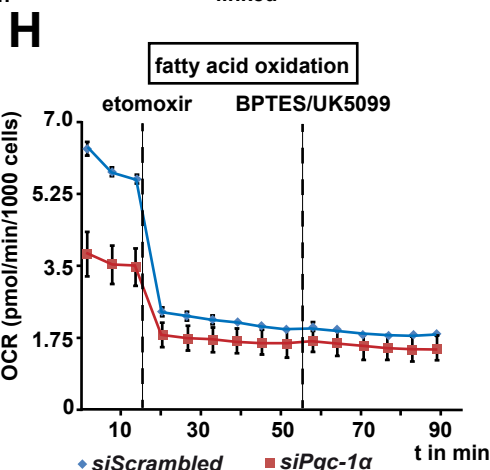
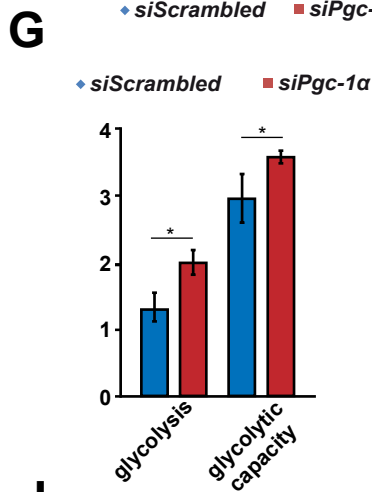
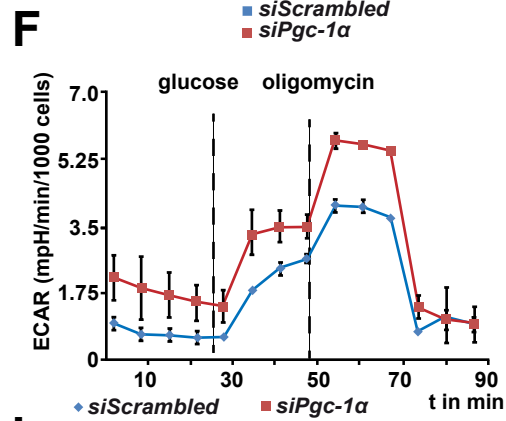
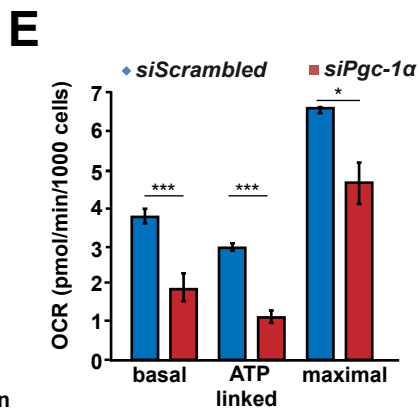
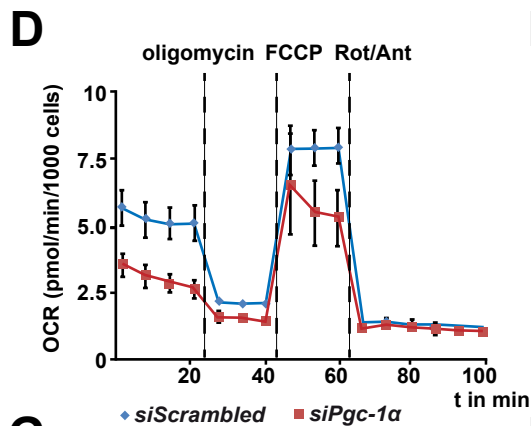
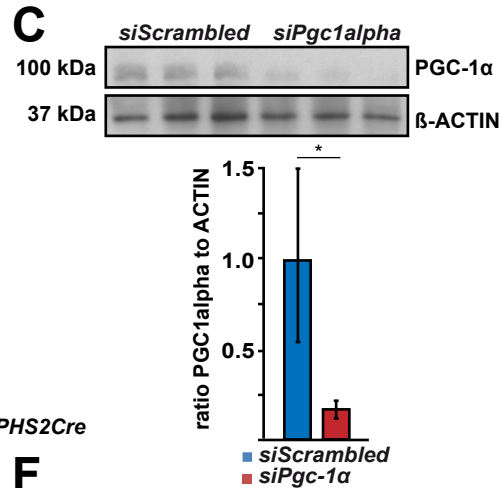
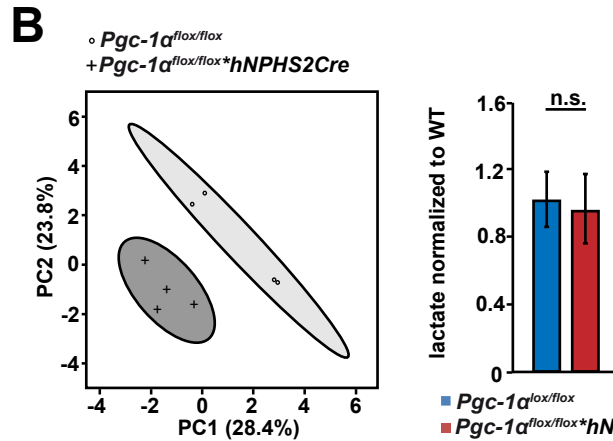
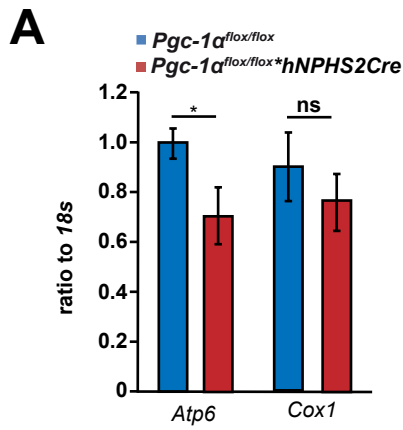


Figure S3: Impact of *Pgc-1 $\alpha$*  deletion on the expression of mitochondria encoded genes and function, Related to Figure 5

(A) qPCR for the abundance of mitochondrial DNA (Atp6, Cox I) normalized to genomic DNA (18s) (p-value \*  $\leq 0.05$ ).

(B) Principal component analysis of metabolite abundance from kidney cortex obtained from 24-week-old mice of respective genotype assessed by unbiased GC-MS based metabolomic analysis (n=4 each group). Lactate levels normalized to WT.

(C) Western blot and densitometry for the abundance of PGC-1 $\alpha$  in human podocytes after siRNA-based knock-down compared to scrambled siRNA controls (p-value \*  $\leq 0.05$ ).

(D) Mitochondrial function of human podocytes after knock-down of *Pgc-1 $\alpha$*  and respective controls. Oxygen consumption rate (OCR) was measured at basal level and after the sequential addition of oligomycin (1 mM), FCCP (0.5 mM), and rotenone (Rot; 1.0 mM) + antimycin A (Ant; 1.0 mM; n=3, technical replicates).

(E) Combined results underline the major role of *Pgc-1 $\alpha$*  for mitochondrial respiratory function as shown for basal respiration, ATP-linked oxygen consumption rate and maximal respiratory capacity (p-value \*  $\leq 0.05$  and \*\*\*  $\leq 0.001$ ).

(F) Extracellular acidification rate (ECAR) of human podocytes with knock-down of *Pgc-1 $\alpha$*  and respective controls at baseline and after injection of glucose followed by oligomycin.

(G) Combined results underline the major impact of *Pgc-1 $\alpha$*  for anaerobic utilization of glucose as shown for glycolysis and maximal glycolytic capacity (p-value \*  $\leq 0.05$ ).

(H) Dependency of fatty acid oxidation of human podocytes with knock-down for *Pgc-1 $\alpha$*  and respective controls obtained after etomoxir and BPTES/UK5099 injection. Final concentrations: etomoxir: 100  $\mu$ M, BPTES: 30  $\mu$ M, UK5099: 30  $\mu$ M.

(I) Capacity of fatty acid oxidation of human podocytes with knock-down for *Pgc-1 $\alpha$*  and respective controls obtained after BPTES/UK5099 injection followed by etomoxir, Final concentrations: etomoxir: 100  $\mu$ M, BPTES: 30  $\mu$ M, UK5099: 30  $\mu$ M.

(J) Dependency of pyruvate oxidation of human podocytes with knock-down for *Pgc-1 $\alpha$*  and respective controls obtained after UK5099 and BPTES/etomoxir injection. Final concentrations: UK5099: 30  $\mu$ M, etomoxir: 100  $\mu$ M, BPTES: 30  $\mu$ M.

(K) Capacity of pyruvate oxidation of human podocytes with knock-down for *Pgc-1 $\alpha$*  and respective controls obtained after BPTES/etomoxir and UK5099 injection. Final concentrations: etomoxir: 100  $\mu$ M, BPTES: 30  $\mu$ M, UK5099: 30  $\mu$ M.

(L) Dependency of glutamine oxidation of human podocytes with knock-down for *Pgc-1 $\alpha$*  and respective controls obtained after BPTES and UK5099/etomoxir injection. Final concentrations: BPTES: 30  $\mu$ M, UK5099: 30  $\mu$ M, etomoxir: 100  $\mu$ M.

(M) Capacity of glutamine oxidation of human podocytes with knock-down for *Pgc-1 $\alpha$*  and respective controls obtained after UK5099/etomoxir and BPTES injection. Final concentrations: UK5099: 30  $\mu$ M, etomoxir: 100  $\mu$ M, BPTES: 30  $\mu$ M.

(N) Statistics for substrate dependency of human podocytes with knock-down for *Pgc-1 $\alpha$*  and respective controls.

(O) Statistics for substrate capacity of human podocytes with knock-down for *Pgc-1 $\alpha$*  and respective controls.

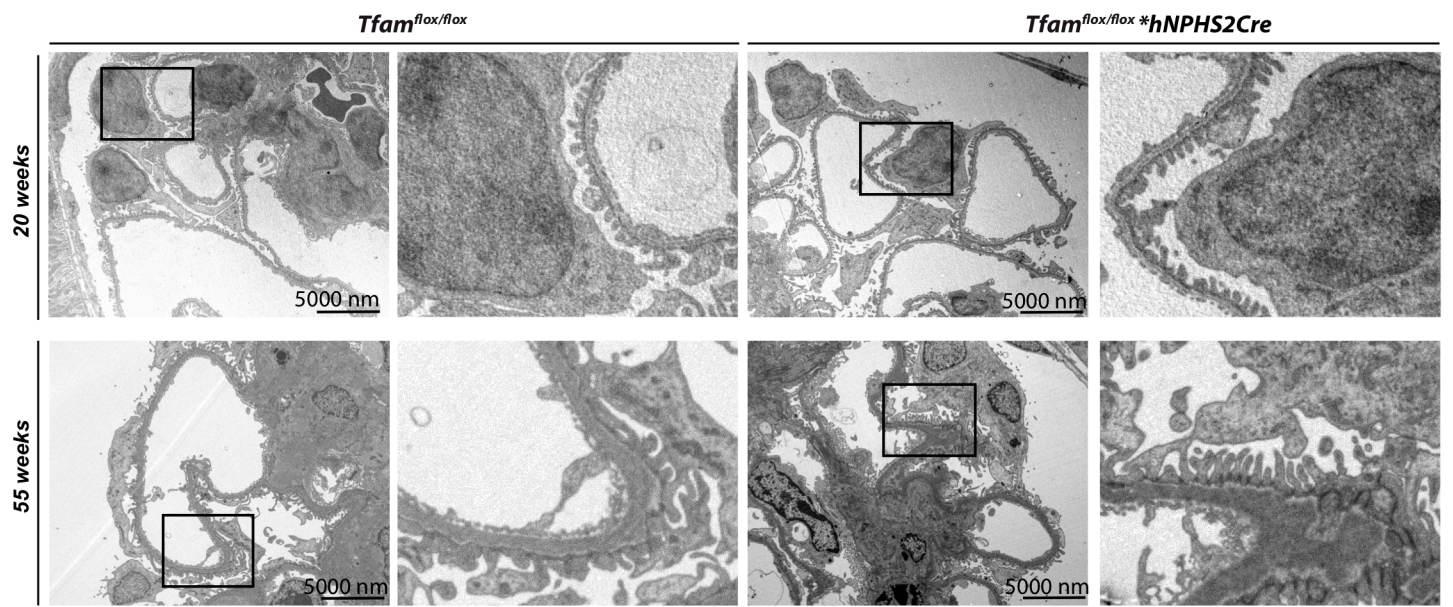
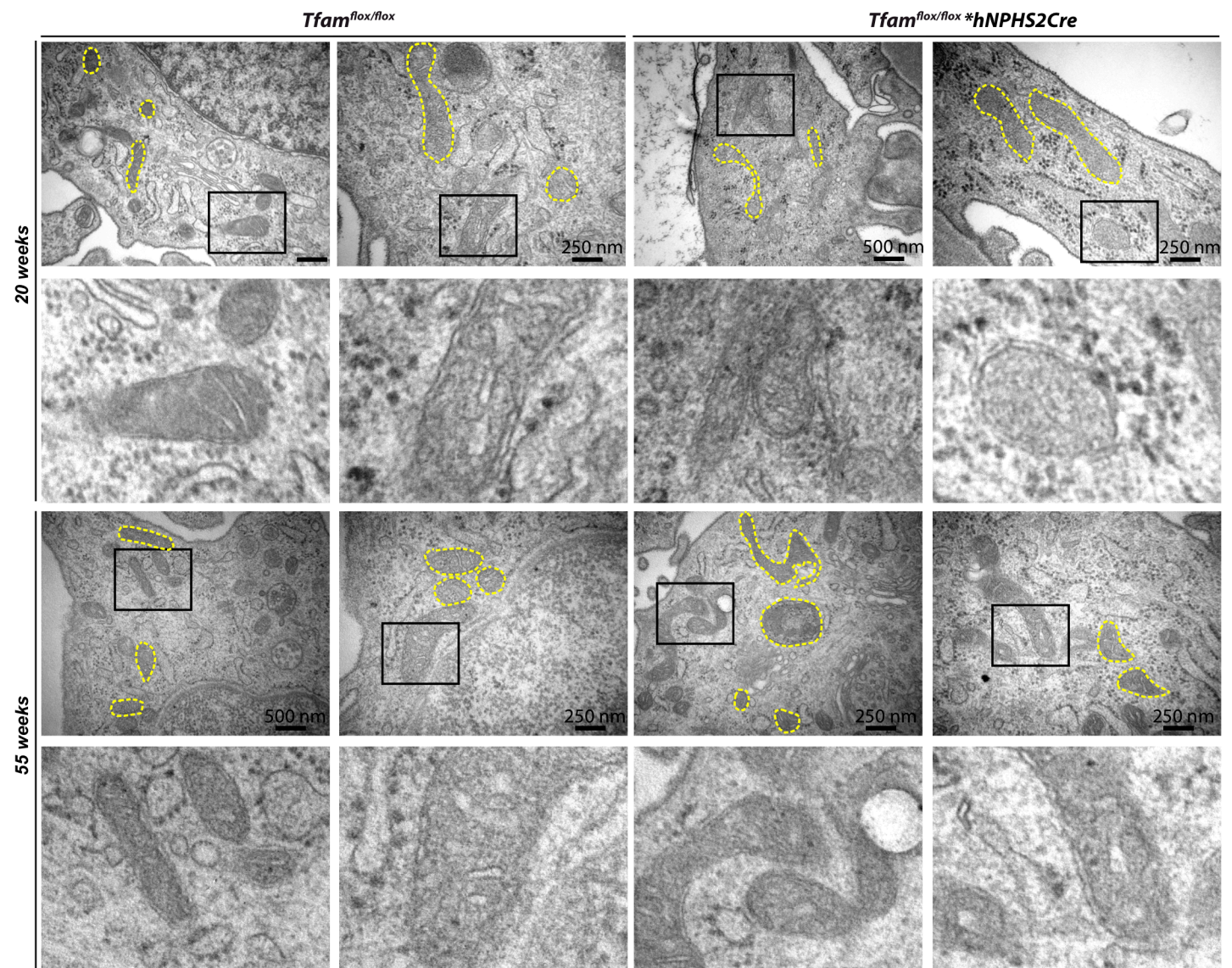
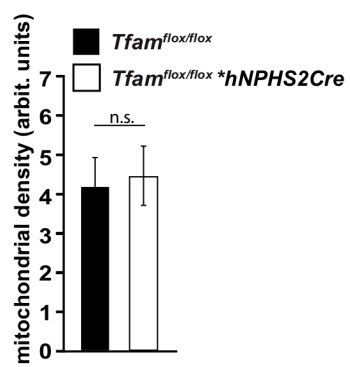
**A****B****C**

Figure S4: Podocyte-specific *Tfam* knockout mice do not develop glomerular disease, Related to Figure 6

Podocyte-specific *Tfam* knockout mice do not develop glomerular disease.

(A) TEM images obtained from 20- and 55 weeks-old *Tfam*<sup>fllox/fllox</sup>\**hNPHS2Cre* and littermate controls show normal foot process formation (representative pictures).

(B) TEM images obtained from 20- and 55 weeks-old *Tfam*<sup>fllox/fllox</sup>\**hNPHS2Cre* and littermate controls showing maintained mitochondrial morphology.

(C) Mitochondrial density in podocytes of *Tfam*<sup>fllox/fllox</sup>\**hNPHS2Cre* and littermate controls (based quantitative analysis of 48 TEM pictures obtained from 4 mice of each genotype, mean ± SD).

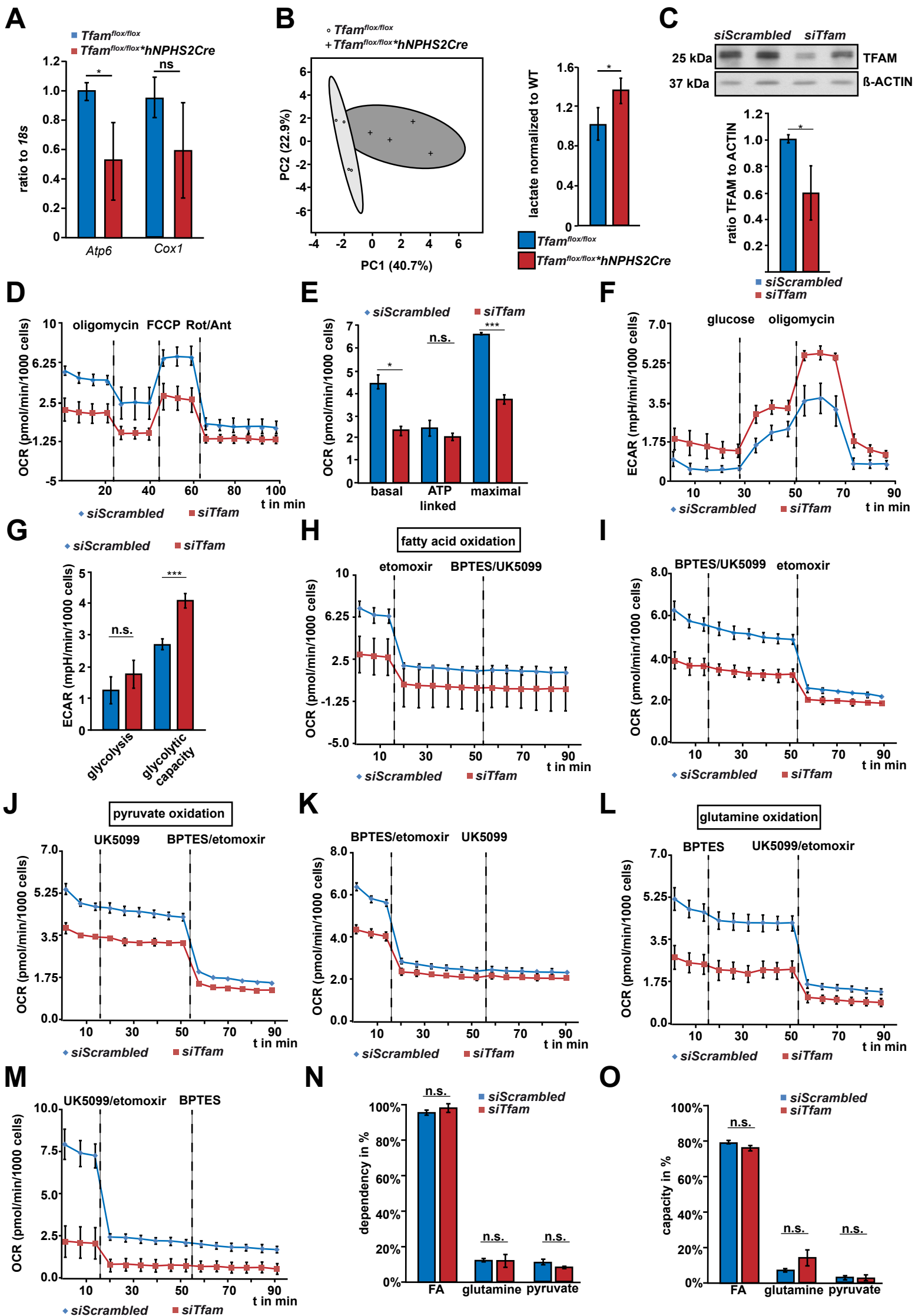


Figure S5: Impact of *Tfam* deletion on the expression of mitochondria encoded genes and function, Related to Figure 6

(A) qPCR for the abundance of mitochondrial DNA (Atp6, Cox I) normalized to genomic DNA (18s) (p-value \*  $\leq 0.05$ ).

(B) Principal component analysis of metabolite abundance from kidney cortex obtained from 24-week-old mice of respective genotype assessed by unbiased GC-MS based metabolomic analysis (n=4 each group). Lactate levels normalized to WT (p-value \*  $\leq 0.05$ ).

(C) Western blot and densitometry for the abundance of TFAM in human podocytes after siRNA-based knock-down compared to scrambled siRNA controls (p-value \*  $\leq 0.05$ ).

(D) Mitochondrial function of human podocytes after knock-down of *Tfam* and respective controls. Oxygen consumption rate (OCR) was measured at basal level and after the sequential addition of oligomycin (1 mM), FCCP (0.5 mM), and rotenone (Rot; 1.0 mM) + antimycin A (Ant; 1.0 mM; n=3, technical replicates).

(E) Combined results underline the major role of *Tfam* for mitochondrial respiratory function as shown for basal respiration, ATP-linked oxygen consumption rate and maximal respiratory capacity (p-value \*  $\leq 0.05$  and \*\*\*  $\leq 0.001$ ).

(F) Extracellular acidification rate (ECAR) of human podocytes with knock-down of *Tfam* and respective controls at baseline and after injection of glucose followed by oligomycin.

(G) Combined results underline the major impact of *Tfam* for anaerobic utilization of glucose as shown for glycolysis and maximal glycolytic capacity (p-value \*  $\leq 0.05$  and \*\*\*  $\leq 0.001$ ).

(H) Dependency of fatty acid oxidation of human podocytes with knock-down for *Tfam* and respective controls obtained after etomoxir and BPTES/UK5099 injection. Final concentrations: etomoxir: 100  $\mu$ M, BPTES: 30  $\mu$ M, UK5099: 30  $\mu$ M.

(I) Capacity of fatty acid oxidation of human podocytes with knock-down for *Tfam* and respective controls obtained after BPTES/UK5099 injection followed by etomoxir, Final concentrations: etomoxir: 100  $\mu$ M, BPTES: 30  $\mu$ M, UK5099: 30  $\mu$ M.

(J) Dependency of pyruvate oxidation of human podocytes with knock-down for *Tfam* and respective controls obtained after UK5099 and BPTES/etomoxir injection. Final concentrations: UK5099: 30  $\mu$ M, etomoxir: 100  $\mu$ M, BPTES: 30  $\mu$ M.

(K) Capacity of pyruvate oxidation of human podocytes with knock-down for *Tfam* and respective controls obtained after BPTES/etomoxir and UK5099 injection. Final concentrations: etomoxir: 100  $\mu$ M, BPTES: 30  $\mu$ M, UK5099: 30  $\mu$ M.

(L) Dependency of glutamine oxidation of human podocytes with knock-down for *Tfam* and respective controls obtained after BPTES and UK5099/etomoxir injection. Final concentrations: BPTES: 30  $\mu$ M, UK5099: 30  $\mu$ M, etomoxir: 100  $\mu$ M.

(M) Capacity of glutamine oxidation of human podocytes with knock-down for *Tfam* and respective controls obtained after UK5099/etomoxir and BPTES injection. Final concentrations: UK5099: 30  $\mu$ M, etomoxir: 100  $\mu$ M, BPTES: 30  $\mu$ M.

(N) Statistics for substrate dependency of human podocytes with knock-down for *Tfam* and respective controls.

(O) Statistics for substrate capacity of human podocytes with knock-down for *Tfam* and respective controls.

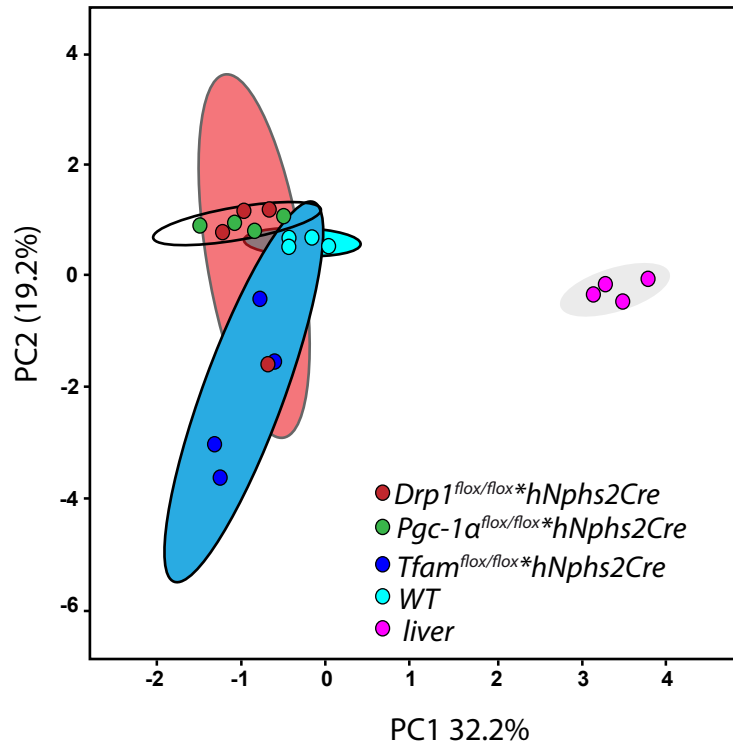
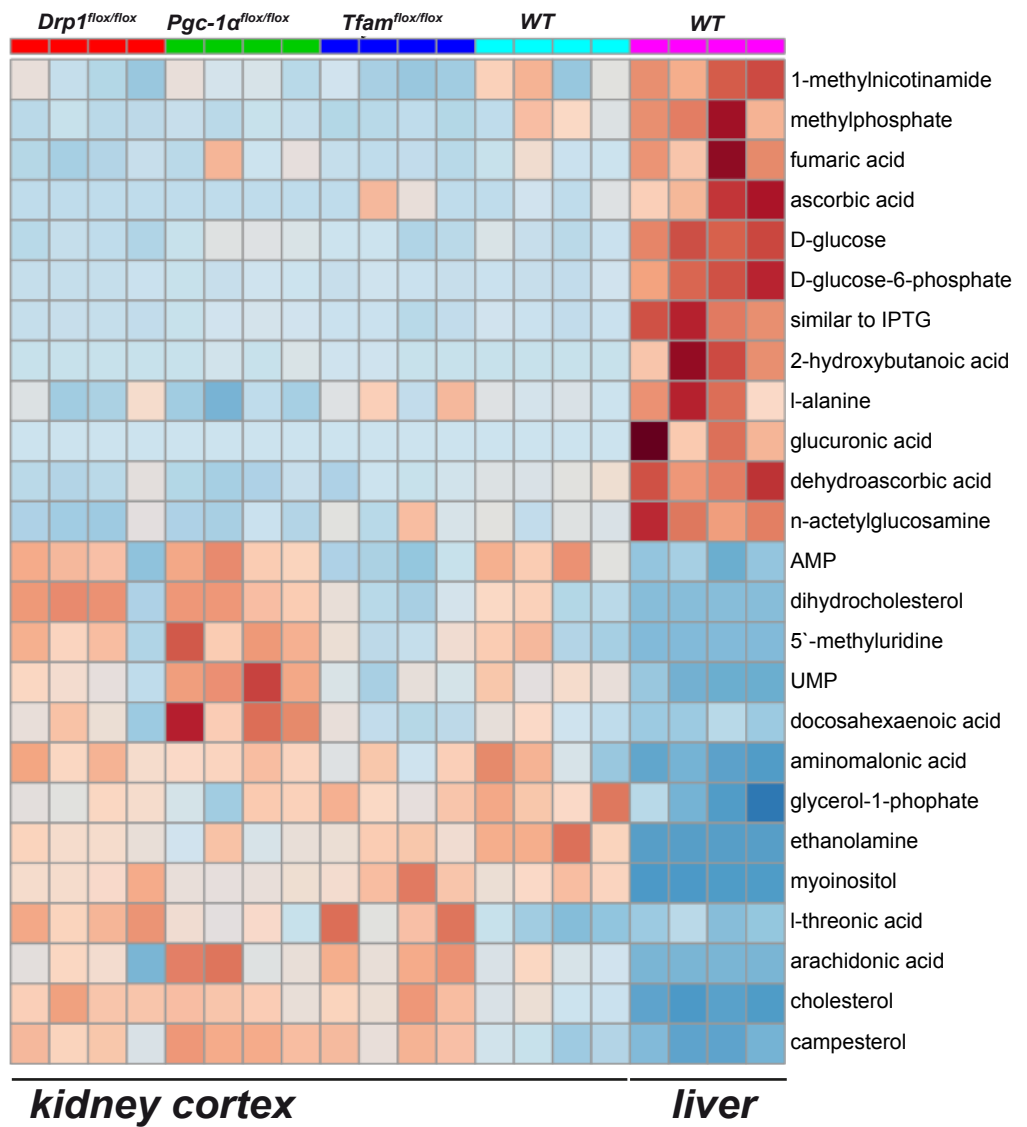
**A****B**

Figure S6: Metabolic profiling of ex vivo isolated kidney cortex of *Drp1*, *Pgc-1 $\alpha$*  and *Tfam* mice, Related to Figure 7

(A) Principal component analysis of metabolites found in kidney cortex of respective genetic mouse models and liver tissue (n=4 each).

(B) Heat map of top 25 significantly different metabolites found in kidney cortex of respective genetic mouse models and liver tissue (n=4 each).